

# Investigation of AC losses in horizontally parallel HTS tapes

Boyang Shen<sup>1</sup>, Jing Li<sup>1</sup>, Jianzhao Geng<sup>1</sup>, Lin Fu<sup>1</sup>, Xiuchang Zhang<sup>1</sup>, Heng Zhang<sup>1</sup>, Chao Li<sup>1</sup>,  
 Francesco Grilli<sup>2</sup>, and T. A. Coombs<sup>1</sup>

<sup>1</sup>Electrical Engineering Division, Department of Engineering, University of Cambridge, Cambridge CB3 0FA, U.K.

<sup>2</sup>Institute for Technical Physics, Karlsruhe Institute of Technology (KIT), 76131 Karlsruhe, Germany.

E-mail: bs506@cam.ac.uk, tac1000@cam.ac.uk

## Abstract

This paper presents an AC loss study of horizontally parallel HTS tapes. We proposed to use three parallel HTS tapes as an example. The AC losses of the middle and end tape of three parallel tapes have been measured using the electrical method and compared to those of an individual tape. The effect of the interaction between tapes on AC losses has been analysed, and compared with finite-element method (FEM) simulations using the 2D  $\mathbf{H}$ -formulation implemented in COMSOL Multiphysics. By using FEM simulations, the cases of increasing number of parallel tapes have been considered, and the normalised ratio between the total average AC losses per tape and the AC losses of an individual single tape has been calculated for different gap distances. We proposed a new parameter,  $N_s$ , a turning point for number of tapes, to divide Stage 1 and Stage 2 for the AC loss study of horizontally parallel tapes. For Stage 1,  $N < N_s$ , the total average losses per tape increased with the increasing number of tapes. For Stage 2,  $N > N_s$ , the total average losses per tape started to decrease with the increasing number of tapes. The analysis demonstrates that horizontally parallel HTS tapes could be potentially used into superconducting devices like HTS transformer, which could retain or even reduce the total average AC losses per tape with large number of parallel tapes.

Keywords: High Temperature Superconductor (HTS), HTS tape, Parallel tape, AC loss.

## 1. Introduction

Superconducting coils fabricated from high temperature superconductor (HTS) are capable of carrying tremendous electrical current density and of creating favourable magnetic field, to be used in various superconducting applications such as Magnetic Resonance Imaging (MRI), superconducting motors [1], and even for superconducting wireless power transmissions [2-8]. However, when HTS applications are operating with alternating current (AC), superconductors also sustain AC losses [9]. AC losses generate heat dissipation, which can create problems in cryogenic systems, and decrease the overall electric power efficiency [10]. Therefore, it is necessarily crucial to consider ways to reduce AC losses and improve the overall power efficiency.

The racetrack and round HTS coils are the most common topologies used in many superconducting applications. In these coils, layers of HTS tape are closely packed, and carry current in the same direction. When observed from a 2D cross-section of the HTS coil, the tapes are stacked on top of each other. This configuration gives rise to large AC losses [11], which are due to the concentration of the perpendicular component of the magnetic field impinging on the HTS tapes [12]. That is the main reason why the AC losses in each turn of the HTS coil are larger than the AC losses in an equivalent single layer of HTS tape.

It is therefore interesting to utilise the geometry of

horizontally parallel HTS tapes (shown in figure 1, sometime also indicated as x-array), which is a proper way to prevent the high AC losses, due to the reduction of the perpendicular component of the magnetic field experienced by the tapes. The parallel HTS tape structure has been reported to potentially reduce the total AC losses in HTS power application such as superconducting transformers [13].

In the literature there are several works dedicated to the AC losses of interacting parallel tapes. Müller [14] and Brambilla et al [15] proposed analytical and numerical solutions for an x-array composed of an infinite number of tapes, respectively. Nakamura et al. performed an AC loss study of YBCO adjacent tapes [16]. Jiang et al. measured the transport AC losses in single and double layer parallel HTS tape arrays [17]. Lee et al. investigated the AC loss of parallel tapes with unbalanced current distribution [13]. Ogawa et al. measured

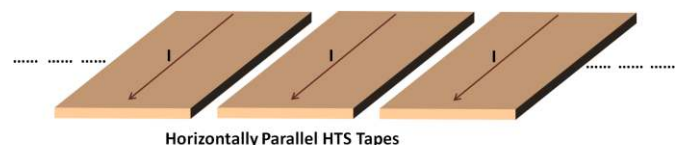
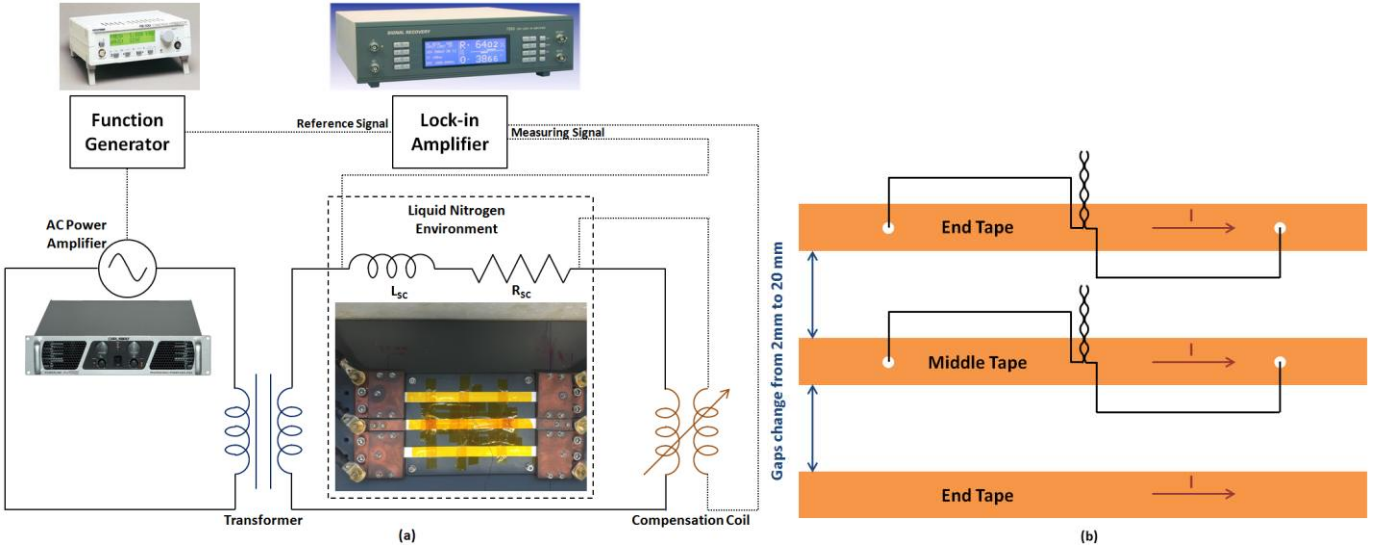


Figure 1. Configuration of multiple horizontally parallel HTS tapes.



**Figure 2.** (a) Experimental schematic of AC loss measurements using electrical method, (b) Graphical instruction of AC loss measurements on parallel HTS tapes.

and simulated the AC losses from an assembled conductor whose configuration was built as parallel HTS tapes [18]. There are other works regarding AC losses of two interacting parallel tapes [19, 20]. However, to the best of our knowledge, in the literature there is no detailed comparison of experiments and simulations for the AC losses of horizontally parallel tapes. A calculation of the AC losses for the case of large but finite number of tapes is also missing. This paper proposes the concept of using horizontally parallel HTS tapes, schematically illustrated in figure 1. Firstly, we used the three horizontally parallel tapes as the basic configuration, and each parallel tape carried the current with same amplitude and direction. Secondly, we set up the experiment of this three-tape configuration and measured the AC losses from both middle and end tapes with increasing gap distance. These measurements were compared with  $H$ -formulation COMSOL simulations. Then, we proposed a new parameter,  $N_s$ , a turning point for number of tapes, to divide Stage 1 and Stage 2 for the AC loss study of horizontally parallel tapes. For Stage 1,  $N < N_s$ , the total average losses per tape increased with the increasing number of tapes. For Stage 2,  $N > N_s$ , the total average losses per tape began to decrease with the increasing number of tapes. By using simulation from COMSOL, we modelled the cases of increasing parallel tapes, and then proposed an empirical relation for the total average AC losses per tape in Stage 1. We have also simulated larger numbers of parallel tapes to verify the approximate value of  $N_s$ . Finally, we analysed the physical reason of why an  $N_s$  existed, and compared our results with Jiang et al's study on x-array HTS tapes [17].

## 2. Experiment Set-up

### 2.1 AC loss measurements by electrical method

Figure 2(a) presents the schematic of the electrical method used to measure the AC losses on HTS tapes. The function generator (digimess® FG100) generated identical AC small signals as the reference input of the lock-in amplifier (Signal

Recovery 7265), and the same AC small signal was amplified by a power amplifier (Carlsbro Powerline Pro 1200) for the primary circuit. The AC current in secondary circuit was increased 16 times by using a step-down transformer. In the secondary side, HTS tapes were immersed into liquid nitrogen at 77 K. The current was calculated using the voltage across the shunt resistor divided by the resistance. The AC currents in both the primary side and secondary side were monitored by a high accuracy data acquisition card linked to the PC with the software NI SignalExpress.

A compensation coil was built by two co-axis coils (first coil for high current side with thick copper cable, and second coil for measuring signal side with thin measurement wire). The compensation coil was used to compensate the inductive signal and then the lock-in amplifier was used to extract the voltage in-phase with the current. The transport AC losses can be calculated as [21]:

$$Q_{ac\_loss} = \frac{I_{rms} \cdot V_{rms}}{f} \quad (1)$$

where  $f$  is the frequency of the AC current,  $I_{rms}$  is the AC transport current flowing through the HTS tape, and  $V_{rms}$  is the in-phase voltage with current  $I_{rms}$ .

### 2.2 AC loss measurements on middle and end tapes

The HTS tapes used in this experiment are SuperPower SF12100 (stabilizer-free), 12 mm wide. The self-field critical current  $I_c$  was measured to be approximately 300 A. As shown in figure 2(a), in the secondary side, three horizontally parallel HTS tapes (20 cm length) were fixed on a plastic board, with the aid of low temperature KAPTON tapes. The tapes were connected in series. The copper cables for the series connection were far away from the tapes (in order to reduce their field effect on the tapes) and are not shown in figure 2(a).

Figure 2(b) schematically illustrates the wiring for AC loss measurements on parallel HTS tapes. First, we started to measure the AC losses in the middle tape, with the distance of each tape's gap increased from 2 mm to 20 mm, and then we did the same AC loss measurements on the end tape. For both

TABLE I  
PARAMETERS FOR THE SIMULATION OF SUPERPOWER SF12100 TAPE

Parameters	Value
Tape width	12 mm
Superconducting layer thickness	1 $\mu\text{m}$
$\mu_0$	$4\pi \times 10^{-7}$ H/m
$n$ (E-J Power Law factor)	25
$J_{c0}$	$2.5 \times 10^{10}$ A/m <sup>2</sup>
$E_0$	$10^{-4}$ V/m
Gap of tapes	2, 4, 6, 8, 10, 12, 14, 16, 18, 20 mm

middle and end tape measurement, the length between two voltage taps was 90 mm. The measuring technique of “8” glyph potential leads was used in order to effectively reduce the noise [22].

### 3. Simulation Method

#### 3.1 $\mathbf{H}$ -formulation

In order to calculate the losses from HTS tape under the action of AC current and AC magnetic field, the  $\mathbf{H}$ -formulation is chosen as the suitable FEM method, which is able to compute the hysteresis losses, ferromagnetic losses and eddy-current losses for different layers of HTS tape [9].  $\mathbf{H}$ -formulation consists of Faraday’s Law (2), Ampere’s Law (3), Ohm’s Law (4), constitutive Law (5), and  $E$ - $J$  power Law (6) [23, 24]:

$$\nabla \times \mathbf{E} = -\frac{\partial \mathbf{B}}{\partial t} \quad (2)$$

$$\nabla \times \mathbf{H} = \mathbf{J} \quad (3)$$

$$\mathbf{E} = \rho \mathbf{J} \quad (4)$$

$$\mathbf{B} = \mu_0 \mu_r \mathbf{H} \quad (5)$$

$$\mathbf{E} = E_0 \left( \frac{\mathbf{J}}{J_c} \right)^n \quad (6)$$

Where  $\mathbf{E}$  is the electric field,  $\mathbf{B}$  is the magnetic flux density,  $\mathbf{H}$  is the magnetic field intensity,  $\mathbf{J}$  is the current density,  $\rho$  is the resistivity,  $\mu_0$  is the permeability of free space,  $\mu_r$  is the relative permeability. Equation (6) is the general  $E$ - $J$  power law for HTS formulation, where  $E_0$  is the characteristic electric field,  $J_c$  is the critical current density and  $n$  is the power factor. By combining equation (2), (3), (4), (5) and (6), the general form of partial differential equation (PDE) for variables  $\mathbf{H}$  to be computed by COMSOL Multiphysics is:

$$\frac{\partial(\mu_0 \mu_r \mathbf{H})}{\partial t} + \nabla \times (\rho \nabla \times \mathbf{H}) = 0 \quad (7)$$

#### 3.2 AC loss calculation

In the FEM model, we used the real dimensions of the SuperPower SF12100 tape, with a superconducting layer 1  $\mu\text{m}$  thick. The critical current density in self-field was determined to be  $2.5 \times 10^{10}$  A/m<sup>2</sup>, which was equivalent to the measured critical current 300 A at 77 K. Some relevant simulation parameters are listed in TABLE I. As the SuperPower SF12100 tapes have a non-magnetic substrate, there are no ferromagnetic losses. Furthermore, both the measurement and the relevant simulation were carried out using low frequency AC current at 20 Hz, thus we ignored the small amount of eddy-current AC losses in the substrate and metal layers. Therefore, the hysteresis losses in the superconducting layer

dominated the total AC losses of HTS tape. Consequently, only the real geometry of the superconducting layers of parallel tapes was simulated.

For the modelling of HTS tapes by COMSOL, an anisotropic  $\mathbf{B}$ -dependent critical current model was used [10]:

$$J_c(\mathbf{B}) = \frac{J_{c0}}{\left( 1 + \sqrt{\frac{k^2 \mathbf{B}_{para}^2 + \mathbf{B}_{perp}^2}{B_0^2}} \right)} \quad (8)$$

where  $J_{c0}$  was as the critical current density in the self-field 77 K,  $k = 0.186$  and  $B_0 = 0.426$  were used in (8) [25].

We use the Global constraint from general PDE Physics to inject the desired transport current into the HTS tapes [25]. The magnitude of the transport current  $I_t$  is given by the integration of the current density  $\mathbf{J}$  on the superconducting domain  $\Omega$ :

$$I_t = \int_{\Omega} \mathbf{J} \cdot d\Omega \quad (9)$$

The AC loss of the domain of interest  $\Omega$  can be calculated using the power density ( $\mathbf{E} \cdot \mathbf{J}$ ) integration [26]:

$$Q = \frac{2}{T} \int_{0.5T}^T \int_{\Omega} \mathbf{E} \cdot \mathbf{J} \cdot d\Omega dt \quad (10)$$

where  $T$  is the period of cycle.

## 4 Results and Discussion from Three

### Horizontally Parallel Tapes Case

#### 4.1 Influence of the gap distance on AC losses

The AC transport current applied to three parallel HTS tapes was increased from 60 A to 150 A (peak values). Before the measurement on parallel tapes, the AC losses of an individual single tape were also measured and used for reference.

As demonstrated in figure 3, when the gap distance increased from 2 mm to 20 mm, the AC losses of the middle tape gradually increased. For the case of 2 mm gap, the losses in the middle tape are  $1.99\text{E-}4$  J/cycle/m at peak current 150 A, which is 3 times lower than the losses of the individual tape with the same transport current. When the gap was 4 mm,

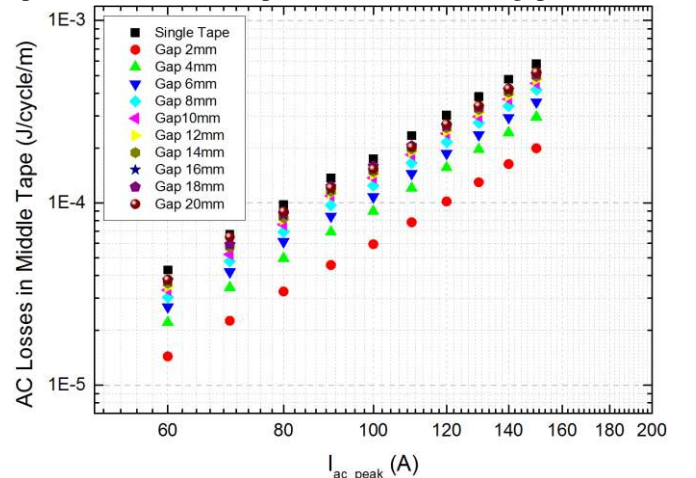


Figure 3. Measured AC losses in the middle tape of the three parallel tapes (Gap changed from 2 mm to 20 mm).

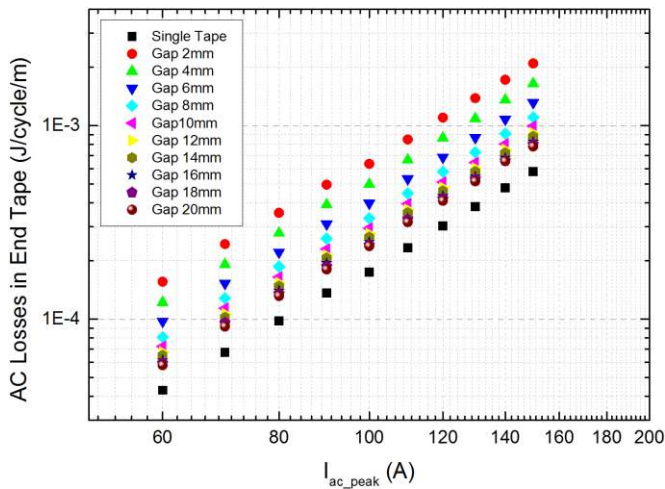


Figure 4. Measured AC losses in the end tape of the three parallel tapes (Gap changed from 2 mm to 20 mm).

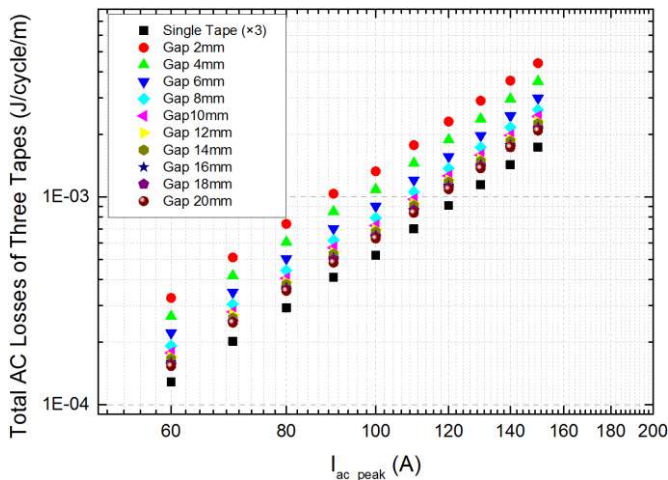


Figure 5. Total measured AC losses from the three parallel tapes (Gap changed from 2 mm to 20 mm).

the AC losses in the middle tape were half ( $2.96\text{E-}4$  J/cycle/m) of those of the individual tape. From 4 mm gap case onward to 20 mm gap case, the changing rate of AC losses in the middle tape became slower.

Figure 4 presents the AC loss measurements on the end tape of three parallel tapes. When the gap distance is 2 mm, the AC losses measured on the end tape were  $2.1\text{E-}3$  J/cycle/m with the transport current 150 A peak, which was more than 3.5 times higher than the losses of the individual tape. With the gap increasing from 2 mm to 20 mm, the AC losses on the end tape started to decrease and to approach the loss value of the individual tape, and the decreasing speed slowed down as well.

As it will be shown later, the reason why the middle tape had lower AC losses than the reference individual one was that the two end tapes created perpendicular magnetic field contributions onto middle tape surface which cancelled each other. However, the end tape had higher AC losses than the reference tape because the middle tape generated a perpendicular magnetic field contribution superposed to that of the end tape. When the gap distance increased to 20 mm, the AC loss features of the middle and end tapes started to approach the individual tape case. Figure 5 illustrates the total

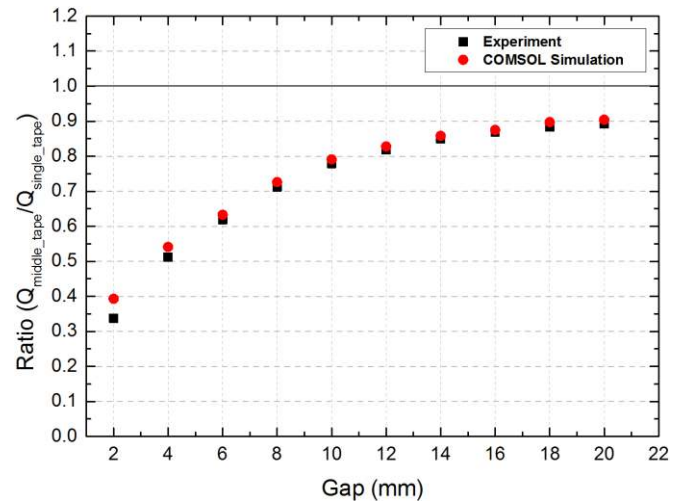


Figure 6. Comparison between simulation and experiment: normalised ratio of middle tape AC losses over the individual single tape AC losses (transport current 150 A at 20 Hz).

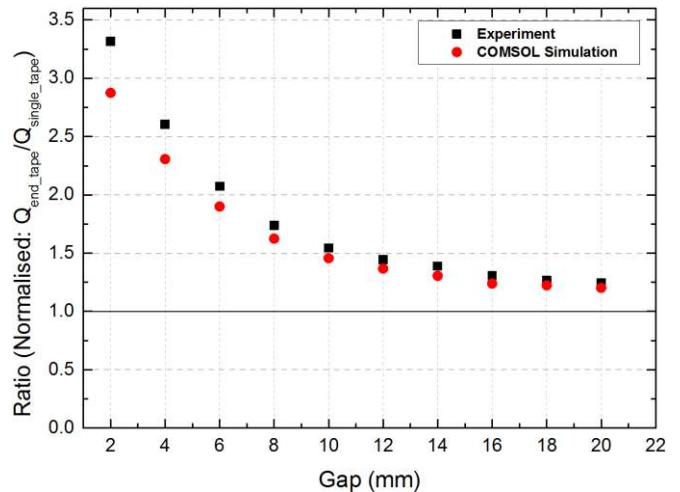
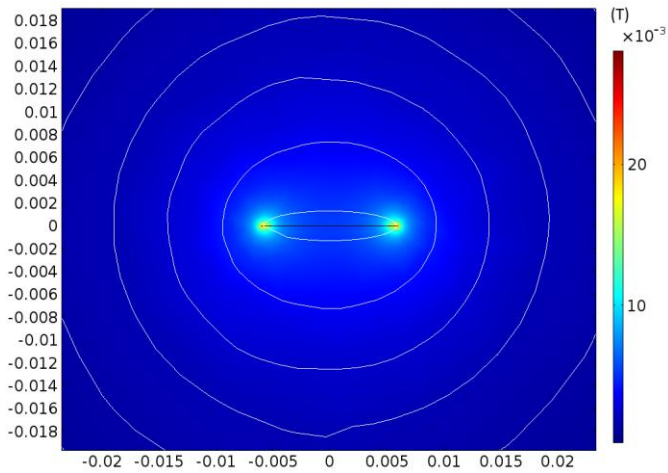


Figure 7. Comparison between simulation and experiment: normalised ratio of end tape AC losses over the individual single tape AC losses (transport current 150 A at 20 Hz).

AC losses of three parallel tapes, which indicates that the total AC losses also decreased when the gap increased. These findings are in agreement with the results for two tapes previously published in the literature [19].

#### 4.2 Comparison between experiment and simulation

For the purpose of investigating the effect of electromagnetic interaction between parallel tapes on their AC losses, first, both the measured and simulation results of an individual tape have been set as the base values. Then, we compared the simulation and experiment based on the normalised ratio of middle/end tape AC losses over the individual single tape AC losses with the different gap distances. Figure 6 presents such comparison for a transport current of 150 A at 20 Hz. In general, there is a good agreement between the experiment and the simulation. However, there were some differences as the parallel tapes with the same direction current attracted each other, which caused the normalised ratio of measured AC losses became smaller than the simulation losses. That was more obvious when the gap distance was relatively small because the attractive effect was stronger with smaller gaps.



**Figure 8.** Magnetic flux density of isolated single tape with 150 A transport current at 20 Hz from COMSOL simulation.

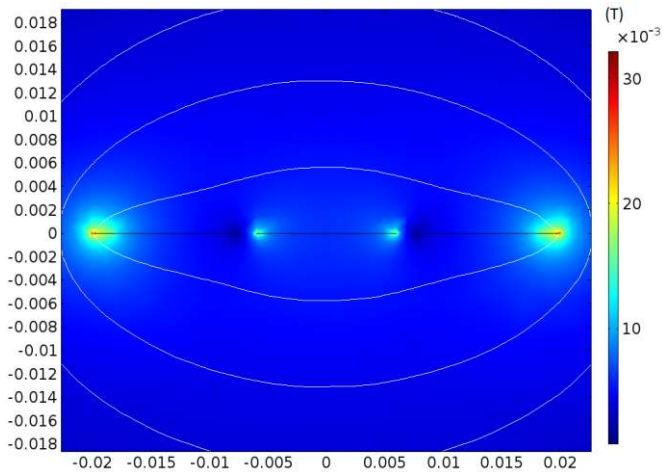


**Figure 9.** Magnetic flux density of 3 parallel tapes with 150 A transport current at 20 Hz from COMSOL simulation (gap distance 2 mm).

A similar phenomenon happened with the end tape, as shown in figure 7. The normalised ratio (experiment and simulation) of the end tape AC losses over the individual tape AC losses was greater with the smaller gaps, such as 2 mm, 4 mm and 6 mm. Figs. 6-7 show a good agreement between experiments and simulations. The differences become noticeable only at small separation gaps (2 mm), and are probably due to local effects (e.g. uniformity of  $J_c$  near the edges, alignment of the tapes) not included in the model. The result and tendency in figure 3-7 are similar to the measurement and calculation in the work from Ogawa et al [18].

Figure 8 and figure 9 illustrate the calculated distributions of the magnetic flux density of the isolated single tape and 3 parallel tapes with 150 A transport current at 20 Hz frequency. In the single tape case (figure 8), the magnetic flux density was greater near the two edges of tape, and thus the AC losses became larger on the two side of tape. Compared with the case of 3 parallel tapes in figure 9, the magnetic flux density around two sides of middle tape was weaker, as two end tapes generated the perpendicular magnetic field cancelling each other, thus effectively shielding the middle tape in between. That was the reason why AC losses were smaller in the middle tape, but with the gap increasing, the shielding effect from two

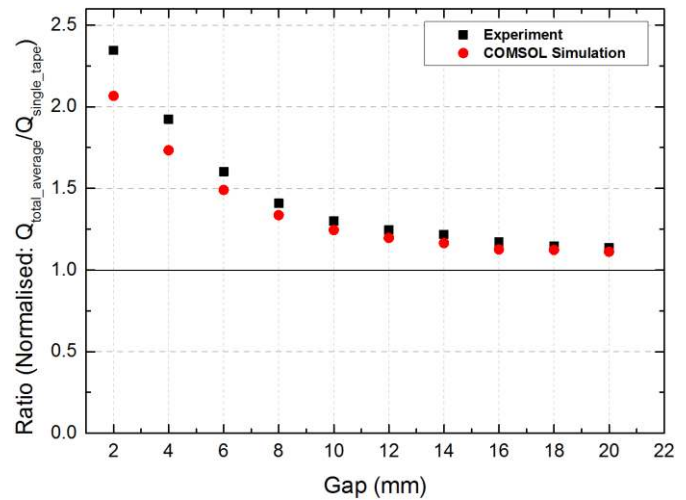


**Figure 10.** Comparison between simulation and experiment: normalised ratio of total average AC losses over the individual single tape AC losses (transport current 150 A at 20 Hz).

end tapes became weaker, and the losses of the middle tape were comparable with losses from each end tape.

## 5 Total Average AC Losses from Increasing Number of Horizontally Parallel Tapes

In order to analyse the efficiency of a certain system, the total AC losses should be considered. For the case of three parallel tapes described in the previous sections, figure 10 presents the comparison of simulation and experiment based on the normalised ratio of total average  $((1 \times \text{Losses}_{\text{mid tape}} + 2 \times \text{Losses}_{\text{end tape}}) / 3)$  AC losses per tape over the individual single tape AC losses. The tendency is similar to the end tape case from figure 7 because the end tape losses dominated the total losses, especially when the gap distances were small. Figure 6, figure 7 and figure 10 demonstrate that the normalised ratios approached unity when the gap increased to higher values, because the interactive effect of parallel tapes on AC losses became less significant. These results are also similar to the work from Jiang et al [17], which was carried out with narrower 4 mm tapes. Generally, the simulation results fit the experiment results as expected.

With the number of parallel tapes increasing, the total loss could consequently increase. However, knowing whether the total average AC loss per tape (total loss/n) would increase or decrease with the increasing number of tapes requires a dedicated investigation. Jiang et al have mentioned in [17] that two regimes can be distinguished: in regime 1 ( $N < N_0$ ), for a small number of tapes in the x-array, the total average AC losses per tape is higher than the AC losses of a single tape, due to the contribution of the tapes situated near the ends of the array; in regime 2 ( $N > N_0$ ), for a large number of tapes in the x-array, the total average AC losses per tape is smaller than the AC losses from a single tape. The relative weigh of the AC losses of the end tapes decreases and the situation resembles gradually that of an infinite x-array, which has been analytically solved by Müller [14].

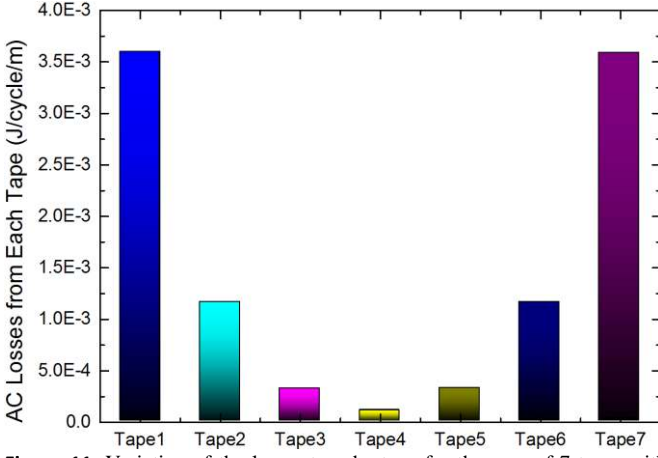


**Figure 11.** Variation of the losses tape-by-tape for the case of 7 tapes with gap distance 2 mm and transport current 150 A at 20 Hz.

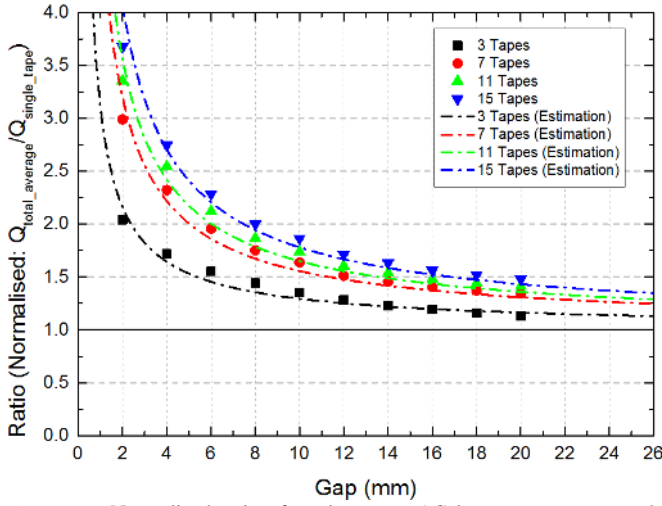


**Figure 12.** Normalized ratio of total average AC losses per tape over the individual single tape AC losses from COMSOL simulation, compared with numerical estimation calculated using Equation (11) and (12) (cases of 3, 7, 11, 15 parallel tapes).

Jiang et al's aforementioned viewpoint is reasonable, and both our experimental and simulation results show that, for a small number of tapes, the total average AC losses per tape are greater than the AC losses of a single tape. In this study, we consider that the transition between Regime 1 and Regime 2 is not a sudden change at a number  $N_0$ . We propose a new parameter,  $N_s$ , a certain number of parallel tapes, to divide Stage 1 and Stage 2. For Stage 1 ( $N < N_s$ ), the total average losses per tape increased with the increasing number of tapes. For Stage 2 ( $N > N_s$ ), the total average losses per tape started to decrease with the increasing number of tapes.

### 5.1 Stage 1 ( $N < N_s$ )-Total average losses per tape

For Stage 1, we have done the experiment and simulation for the case of 3 parallel tapes. Then we tried to simulate cases with more tapes (7, 11, 15). Figure 11 presents the variation of the losses tape-by-tape for the case of 7 tapes with gap distance 2 mm and transport current 150 A at 20 Hz. It can be seen that the losses of the middle tapes were relatively small while the losses of the end tapes still dominated the total AC losses with this small gap (2 mm). As shown in figure 12, the simulations were executed for the case of 3, 7, 11, 15 tapes, and the normalised ratio of total average AC losses per tape

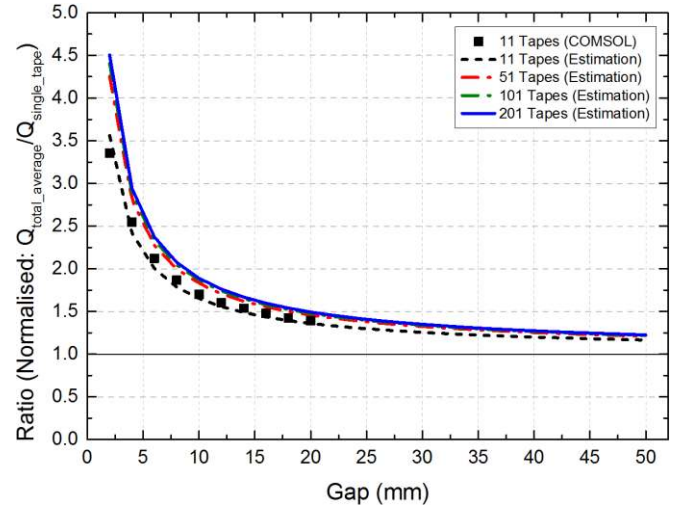


**Figure 13.** Normalised ratio of total average AC losses per tape over the single tape AC losses from Stage 1 numerical estimation calculated using Equation (11) and (12) (cases of 11, 51, 101, 201 parallel tapes), also compared with the COMSOL simulation of 11 parallel tapes case.

over the individual single tape AC losses were calculated with different gap distances. From figure 12, it can be noted that the normalised ratio decreases to approach unity with the increasing gap for all the four cases, and the normalised ratio also kept increasing when the number of parallel tapes went up. However, the increasing rate of normalised ratio slowed down when the number of parallel tapes became higher, which could be seen from the four cases in figure 12.

In order to efficiently find the boundary of Stage 1 other than simulating all cases, an empirical expression for the normalised ratio of total average AC losses over the individual single tape AC losses with different gap distances is proposed for Stage 1 (using a mathematical fitting):

$$Ratio(\text{Normalised}) = a \cdot Gap^b + 1 \quad (11)$$

$$a = c \cdot N^d + e \quad (12)$$

where constants  $b = -0.852$ ,  $c = -9.036$ ,  $d = -0.6212$ , and  $e = 6.66$ . Variable “a” also has the relation with number of parallel tapes “N”. Figure 12 shows the fitting estimations for the cases of 3, 7, 11, 15 tapes, which agree with the COMSOL simulation results. Mathematically, Equation (11) and Equation (12) indicate that the normalised ratio converges to unity not only with increasing gap distance but also with the increasing number of parallel tapes in Stage 1.

Figure 13 presents the numerical estimation calculated by using Equation (11) and (12): the normalised ratio of the total average AC losses over the individual single tape AC losses with gap distances up to 50 mm. We have increased the number of parallel tapes from 11, 51, and 101 to 201. As shown in figure 13, the calculation of 11 tapes agreed with the COMSOL simulation result of 11 tapes. It can be seen from figure 13 that the difference between 11 and 51 tapes cases was quite substantial, while the difference between 51, 101 and 201 tapes cases were fairly small. It could be deduced that the total average AC losses per tape would start to saturate when the number of tapes reaches certain level in Stage 1.

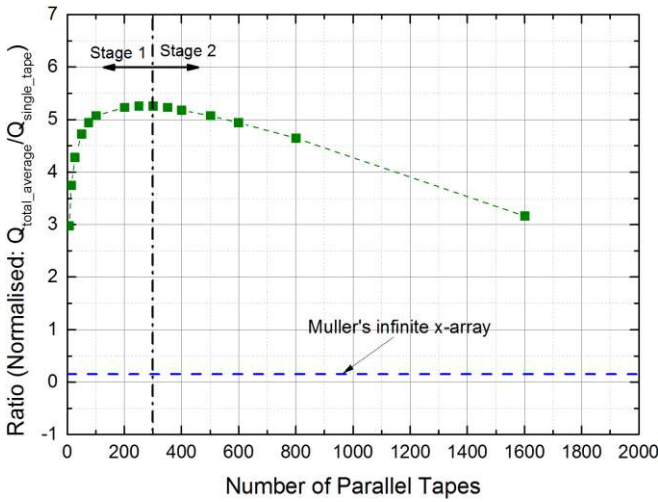


**Figure 14.** Cases of 7, 15, 27, 51, 75, 101, 201, 251, 301, 351, 401, 501, 601, 801, and 1601 parallel tapes with constant gap distance 2 mm and transport current 150 A at 20 Hz using COMSOL simulation, and the analysis of  $N_s$ , Stage 1 and Stage 2, with the reference of Müller's analytical result for infinite tapes.

### 5.2 Stage 2 ( $N > N_s$ )-Total average losses per tape

Based on the numerical relation and simulation results from Stage 1, we expected that the increasing trend of normalised ratio for total average AC losses per tape would saturate for a number of tapes in the order of a few hundreds. Then, we continued to increase the number of parallel tapes with bigger step to discover the value of  $N_s$ . As shown in figure 14, we simulated the cases of 7, 15, 27, 51, 75, 101, 201, 251, 301, 351, 401, 501, 601, 801, and 1601 tapes with constant gap distance 2 mm and transport current 150 A at 20 Hz. It can be seen that the turning point,  $N_s$ , was around the case of 301 tapes (which corresponds to a total width of the array of about 4.2 m). From this point onward, the total average AC losses per tape started to decrease with the further increasing number of parallel tapes. The maximum number of tapes we have simulated is 1601, and for this case the total average AC losses per tape has decreased to a value similar to that of 7 tapes. The normalised ratio of 1601 tape case was still a long way not only from the Müller's infinite x-array with same gap distance (shown with a dashed line in figure 14), but also from the losses of the individual tape.

### 5.3 Summary

Based on the results shown above, we have found that the total average losses per tape would firstly increase, saturate, and then decrease with the incremental number of horizontally parallel tapes. In Stage 1, parallel tapes interact more strongly with each other when the number of tapes was small. Although middle tapes had lower losses than a single tape, the end tapes dominated the total losses because of the strong magnetic fields around them, and the total average losses per tape increased with increasing tapes. There was a turning point,  $N_s$ , dividing the Stage 1 and Stage 2, which could distinguish when the total average losses per tape would increase or decrease with increasing tapes. In Stage 2, when the amount of parallel tapes became higher, the total planar length of tape system was longer, and the far tapes had much less influence. Therefore, the AC losses contributed from the end tapes

started to become less important, and the total average losses per tape began to decrease with increasing tapes.

Jiang et al's conclusion on  $N_0$  is applicable to our study. Comparing  $N_s$  with  $N_0$ ,  $N_0$  should be much greater than  $N_s$ . However, it is difficult to use the FEM simulation to achieve massive amount of tape elements, due to the limitation of PC's computing capability.  $N_s$  could be a useful parameter to determine the turning point where the total average losses per tape start to reduce, which is helpful for designing a system of horizontally parallel tapes.

The AC loss feature of horizontally parallel tapes is different from the stacked tapes in a HTS coil. The total average AC losses per tape still go up observably even when the HTS coil geometry increases to hundreds of turns. The geometry of horizontally parallel tapes could be able to maintain or even reduce the total average losses per tape, especially when the number of parallel tapes increases to high level, and therefore this geometry could be potentially applied to superconducting devices such as HTS transformers.

## 6 Conclusion

A study on AC losses of horizontally parallel HTS tapes has been presented. AC loss measurements on middle and end tape of three parallel tapes have been carried out using the electrical method. The AC losses from individual single tape have also been measured and used as reference. The middle tape had less AC losses than the reference individual tape, due to the reduction of the perpendicular field component at its edges. On the contrary, the end tape had larger AC losses than the reference individual tape due to the substantial perpendicular field component at one of its edges. The interactive effect on AC losses from middle and end tape became less significant when the gap distance increased, and the loss value started to approach that of the individual tape. The simulation of the parallel-tape experiment has been executed by 2D  $H$ -formulation on the FEM platform of COMSOL Multiphysics. The simulation results fit the experimental results on the AC loss features of middle and end tape with the increasing gap distance.

The total average losses per tape of horizontally parallel tapes have been investigated. We have proposed a new parameter,  $N_s$ , which is a number of parallel tapes to divide Stage 1 and Stage 2. In Stage 1,  $N < N_s$ , parallel tapes contributed more interaction to each other and high peak magnetic fields around the end tapes, which caused large AC losses in the end tapes, which dominate the total losses. As a consequence, the total average losses per tape increased with increasing number of tapes. In Stage 2,  $N > N_s$ , the far tapes had much less impact on the total losses as the total planar length of tape system became longer, and the AC losses contributed from the end tapes tended to become relatively negligible. Therefore, the total average losses per tape started to decrease with increasing number of tapes. In order to efficiently find the boundary of Stage 1 other than using COMSOL to simulate all cases, a mathematical relation between the normalised ratio of total average AC losses per tape and different gap distances has been proposed. According

to this expression, the normalised loss ratio converges to one (i.e. the average loss per tape converges to that of an isolated tape) with increasing gap distance, but also with increasing number of parallel tapes. According Jiang et al's study, it could be estimated the total average AC losses would approach the Müller's analytical results for infinite tapes with number of tapes  $N_0$ , but  $N_0$  should be much larger than  $N_s$ . The turning point,  $N_s$ , could be a useful factor to resolve where the total average losses per tape start to reduce, which is beneficial for designing a system of horizontally parallel tapes. The geometry of horizontally parallel tapes could be potentially applied to superconducting devices like HTS transformers, because this structure is able to maintain and even reduce the total average AC losses per tape with large number of tapes.

## 7 Acknowledgments

The experimental work was completed with the help of the Electrical Engineering Division, Department of Engineering, University of Cambridge. Authors would like to express gratitude to Mr John Grundy and other members of staff for their important assistance. Some of the authors are research students, and they are particularly grateful to China Scholarship Council (CSC) for their scholarships and support for overseas study.

## 8 References

- [1] J. R. Hull, "Applications of high-temperature superconductors in power technology," *Reports on Progress in Physics*, vol. 66, no. 11, pp. 1865, 2003.
- [2] G. Zhang, H. Yu, L. Jing, J. Li, Q. Liu, and X. Feng, "Wireless power transfer using high temperature superconducting pancake coils," *IEEE Transactions on Applied Superconductivity*, vol. 24, no. 3, pp. 1-5, 2014.
- [3] I. K. Yoo et al, "Design and Analysis of High Q-Factor LC Resonant Coil for Wireless Power Transfer," *Korean Institute of Information Technology*, pp. 9-116, 2014.
- [4] I.-S. Jeong, H.-S. Choi, and M.-S. Kang, "Application of the Superconductor Coil for the Improvement of Wireless Power Transmission Using Magnetic Resonance," *Journal of Superconductivity and Novel Magnetism*, vol. 28, no. 2, pp. 639-644, 2015.
- [5] I.-S. Jeong, Y.-K. Lee, and H.-S. Choi, "Characteristics analysis on a superconductor resonance coil WPT system according to cooling vessel materials in different distances," *Physica C: Superconductivity and its Applications*, vol. 530, pp. 123-132, 2016.
- [6] H. Yu, G. Zhang, L. Jing, Q. Liu, W. Yuan, Z. Liu, and X. Feng, "Wireless power transfer with HTS transmitting and relaying coils," *IEEE Transactions on Applied Superconductivity*, vol. 25, no. 3, pp. 1-5, 2015.
- [7] W. Zuo, S. Wang, Y. Liao, and Y. Xu, "Investigation of efficiency and load characteristics of superconducting wireless power transfer system," *IEEE Transactions on Applied Superconductivity*, vol. 25, no. 3, pp. 1-6, 2015.
- [8] A. Kurs, A. Karalis, R. Moffatt, J. D. Joannopoulos, P. Fisher, and M. Soljačić, "Wireless power transfer via strongly coupled magnetic resonances," *science*, vol. 317, no. 5834, pp. 83-86, 2007.
- [9] F. Grilli, E. Pardo, A. Stenvall, D. N. Nguyen, W. Yuan, and F. Gömöry, "Computation of losses in HTS under the action of varying magnetic fields and currents," *IEEE Trans. Appl. Supercond.*, vol. 24, no. 1, pp. 78-110, 2014.
- [10] J. Šouc, E. Pardo, M. Vojenčiak, and F. Gömöry, "Theoretical and experimental study of AC loss in high temperature superconductor single pancake coils," *Superconductor Science and Technology*, vol. 22, no. 1, pp. 015006, 2008.
- [11] F. Grilli, and S. P. Ashworth, "Measuring transport AC losses in YBCO-coated conductor coils," *Supercond. Sci. Technol.*, vol. 20, no. 8, pp. 794, 2007.
- [12] E. Pardo, and F. Grilli, "Numerical simulations of the angular dependence of magnetization AC losses: coated conductors, Roebel cables and double pancake coils," *Superconductor Science and Technology*, vol. 25, no. 1, pp. 014008, 2011.
- [13] S. Lee, S. Byun, W. Kim, K. Choi, and H. Lee, "AC loss analysis of a HTS coil with parallel superconducting tapes of unbalanced current distribution," *Physica C: Superconductivity and its applications*, vol. 463, pp. 1271-1275, 2007.
- [14] K.-H. Müller, "AC losses in stacks and arrays of YBCO/hastelloy and monofilamentary Bi-2223/Ag tapes," *Physica C: Superconductivity*, vol. 312, no. 1, pp. 149-167, 1999.
- [15] R. Brambilla, F. Grilli, D. N. Nguyen, L. Martini, and F. Sirois, "AC losses in thin superconductors: the integral equation method applied to stacks and windings," *Superconductor Science and Technology*, vol. 22, no. 7, pp. 075018, 2009.
- [16] S. Nakamura, J. Ogawa, O. Tsukamoto, and U. Balachandran, "AC Transport Current Losses in YBCO Tapes with Adjacent Tapes." pp. 877-884.
- [17] Z. Jiang, N. Long, M. Staines, Q. Li, R. Slade, N. Amemiya, and A. Caplin, "Transport AC loss measurements in single-and two-layer parallel coated conductor arrays with low turn numbers," *IEEE Transactions on Applied Superconductivity*, vol. 22, no. 6, pp. 8200306-8200306, 2012.
- [18] J. Ogawa, S. Fukui, M. Yamaguchi, T. Sato, O. Tsukamoto, and S. Nakamura, "Comparison between experimental and numerical analysis of AC transport current loss measurement in YBCO tapes in an assembled conductor," *Physica C: Superconductivity and its applications*, vol. 445, pp. 1083-1087, 2006.
- [19] Z. S. Wu, Y. R. Xue, J. Fang, Y. J. Huo, and L. Yin, "The influence of the YBCO tape arrangement and gap between the two tapes on AC losses." pp. 205-206.
- [20] K. Ryu, K. Park, and G. Cha, "Effect of the neighboring tape's AC currents on transport current loss of a Bi-2223 tape," *IEEE transactions on applied superconductivity*, vol. 11, no. 1, pp. 2220-2223, 2001.
- [21] W. Yuan, T. A. Coombs, J. H. Kim, C. H. Kim, J. Kvitkovic, and S. Pamidi, "Measurements and calculations of transport AC loss in second generation high temperature superconducting pancake coils," *Journal of Applied Physics*, vol. 110, no. 11, pp. 113906, 2011.
- [22] Y. Zhao, J. Fang, W. Zhang, J. Zhao, and L. Sheng, "Comparison between measured and numerically calculated AC losses in second-generation high temperature superconductor pancake coils," *Phys. C, Supercond.*, vol. 471, no. 21, pp. 1003-1006, 2011.
- [23] Z. Hong, A. M. Campbell, and T. A. Coombs, "Numerical solution of critical state in superconductivity by finite element software," *Supercond. Sci. Technol.*, vol. 19, no. 12, pp. 1246, 2006.
- [24] R. Brambilla, F. Grilli, and L. Martini, "Development of an edge-element model for AC loss computation of high-temperature superconductors," *Superconductor Science and Technology*, vol. 20, no. 1, pp. 16, 2006.
- [25] B. Shen, L. Fu, J. Geng, H. Zhang, X. Zhang, Z. Zhong, Z. Huang, and T. A. Coombs, "Design of a Superconducting Magnet for Lorentz Force Electrical Impedance Tomography," *IEEE Trans. Appl. Supercond.*, vol. 26, no. 3, 2016.
- [26] F. Grilli, V. M. Zermeno, E. Pardo, M. Vojenčiak, J. Brand, A. Kario, and W. Goldacker, "Self-field effects and AC losses in pancake coils assembled from coated conductor Roebel cables," *IEEE Trans. Appl. Supercond.*, vol. 24, no. 3, 2014.